

# 1 **Electronic Supplementary Material**

## 2 **Methods**

### 3 *Phylogeny*

4 I reanalysed sequence data from a thorough investigation of rockfish phylogeny  
5 (see Hyde & Vetter 2007 for methods and GenBank Accession numbers). I used the  
6 program BEAST (<http://beast.bio.ed.ac.uk/>) to produce a time-calibrated tree based on 2  
7 nuclear and 7 mitochondrial genes. I included the biogeographic calibration point used  
8 previously (Hyde & Vetter 2007), with a strong prior (normal, mean 3 m.y.a., s.d. 0.05  
9 m.y.a.) on the divergence time between *Sebastes alutus* and a clade of four Atlantic  
10 species. I also used a weakly informative lognormal prior (mean 7 m.y.a., log s.d. 0.5  
11 m.y.a.) on the root age of *Sebastes* based on the sparse fossil record. I ran the analysis for  
12 20 million generations, sampling every 2500<sup>th</sup> tree for a total of 8000 samples, and  
13 discarded the first 25% as burn-in. I used the ‘TreeAnnotater’ utility to produce the  
14 maximum clade credibility tree (maximizing the sum of the posterior probabilities of  
15 nodes) and to calculate mean branch lengths from the posterior distribution.

16 The full phylogeny included 99 species of *Sebastes* as well as four outgroups  
17 (*Hozukius emblemarius*, *Helicolenus avius*, *Sebastolobus alascanus* and *Sebastiscus*  
18 *marmoratus*). I removed all but the 66 northeast Pacific *Sebastes* species from the tree for  
19 this study, meaning some nodes were missing from the 66 species tree. I did not include  
20 these nodes in the analyses described below, on the grounds that these speciation events  
21 occurred outside the northeast Pacific arena of diversification investigated in this study. I  
22 also excluded three morphologically cryptic species that have been proposed since the  
23 initiation of this study (Hyde & Vetter 2007, Hyde *et al.* 2008, Burford 2009). The

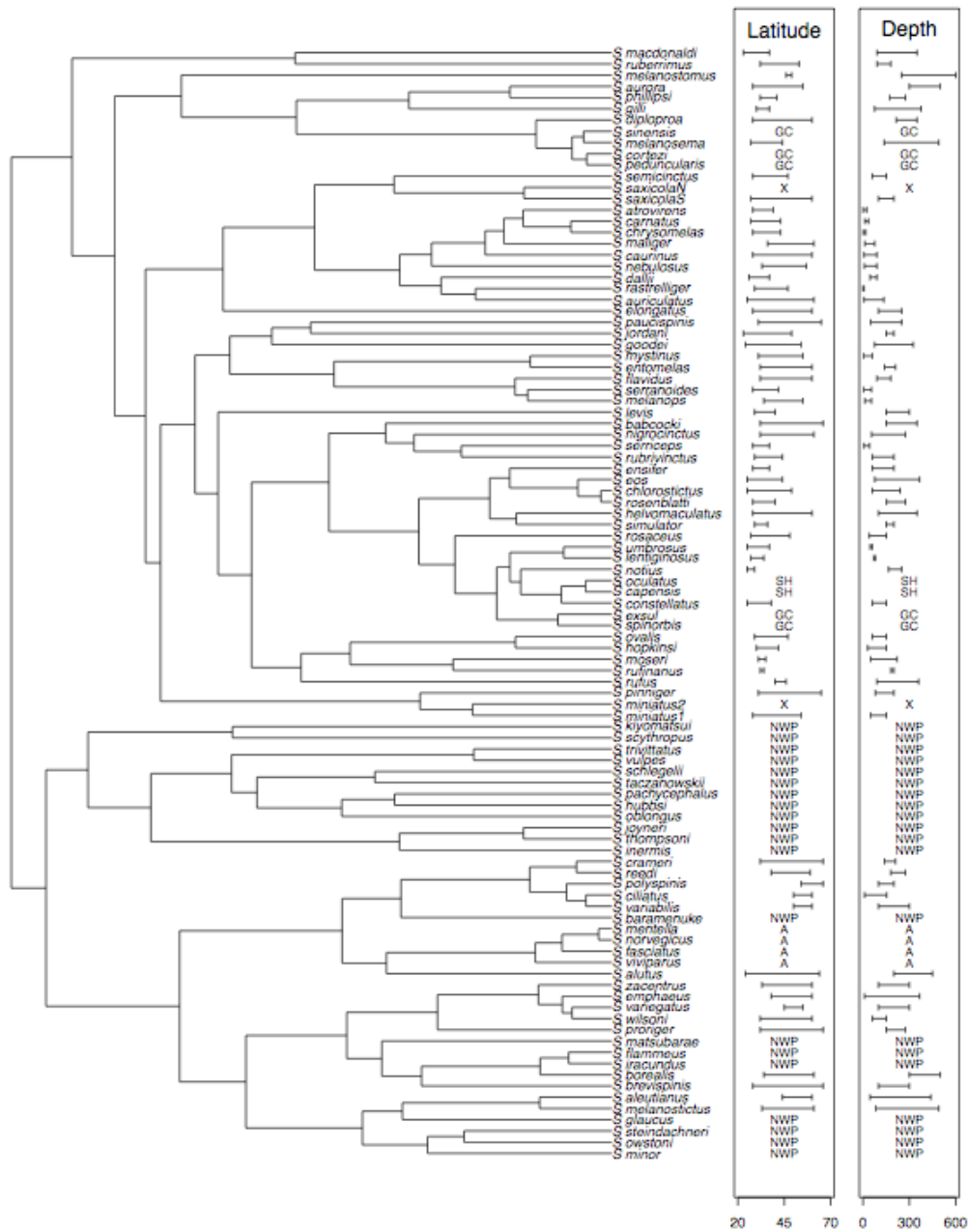
24 resulting tree (fig. S1) was highly similar to a previously published Bayesian consensus  
25 tree (fig. 3 in Hyde & Vetter 2007), with almost perfect congruence near the tips, and  
26 disagreement about earlier nodes largely coming from my decision to resolve all nodes  
27 rather than collapse weakly supported nodes into polytomies.

28

## 29 *Simulations*

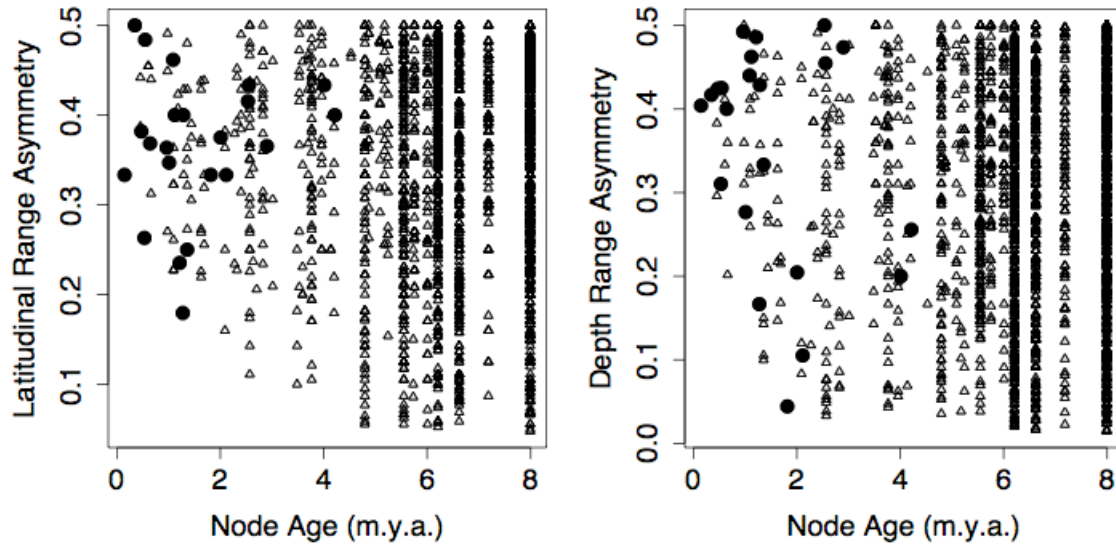
30 To ensure that the inference method can recover known differences in  $\psi$ , I  
31 simulated growth of 66 phylogenetic trees following a birth-death process with  $\lambda = 0.5$   
32 and  $\mu = 0$  or  $0.1$ . Concurrent with tree growth, I simulated character evolution in  
33 accordance with the model assumed in this article, where evolution occurs via both  
34 Brownian motion and step change at speciation. For the 33 trees with a given value of  $\mu$ ,  
35 I simulated character evolution with  $\sigma_t^2 = 0.1$  and three replicates of each of 11 values of  
36  $\psi$  (0, 0.1...0.9, 1). At each time step ( $\Delta t = 0.01$ ), each lineage speciated with probability  
37  $\lambda\Delta t$  or went extinct with probability  $\mu\Delta t$ . Brownian motion evolution occurred at a rate of  
38  $\sigma_a^2\Delta t$ , where  $\sigma_a^2 = \sigma_t^2(1-\psi)$ , and at speciation the change in traits of each daughter  
39 species had variance  $\sigma_c^2$ , where  $\sigma_c^2 = (\sigma_t^2\psi)/\lambda$ . I ran each analysis until the number of  
40 extant species matched the number of species in the rockfish tree ( $N = 66$ ).

41 The inference method consistently recovers purely gradual evolution ( $\psi = 0$ ).  
42 There was no bias in the estimations of higher values of  $\psi$  (0.1-1), though there was  
43 considerable scatter around these estimates ( $R^2$  ranged from 0.6-0.78; fig. S7). There was  
44 no obvious improvement in estimation when the true  $\lambda$  and  $\mu$  were used instead of  $\lambda$  and  
45  $\mu$  estimated from the tree, indicating that the estimation of speciation and extinction rates  
46 does not considerably increase the error in estimates of  $\psi$ .



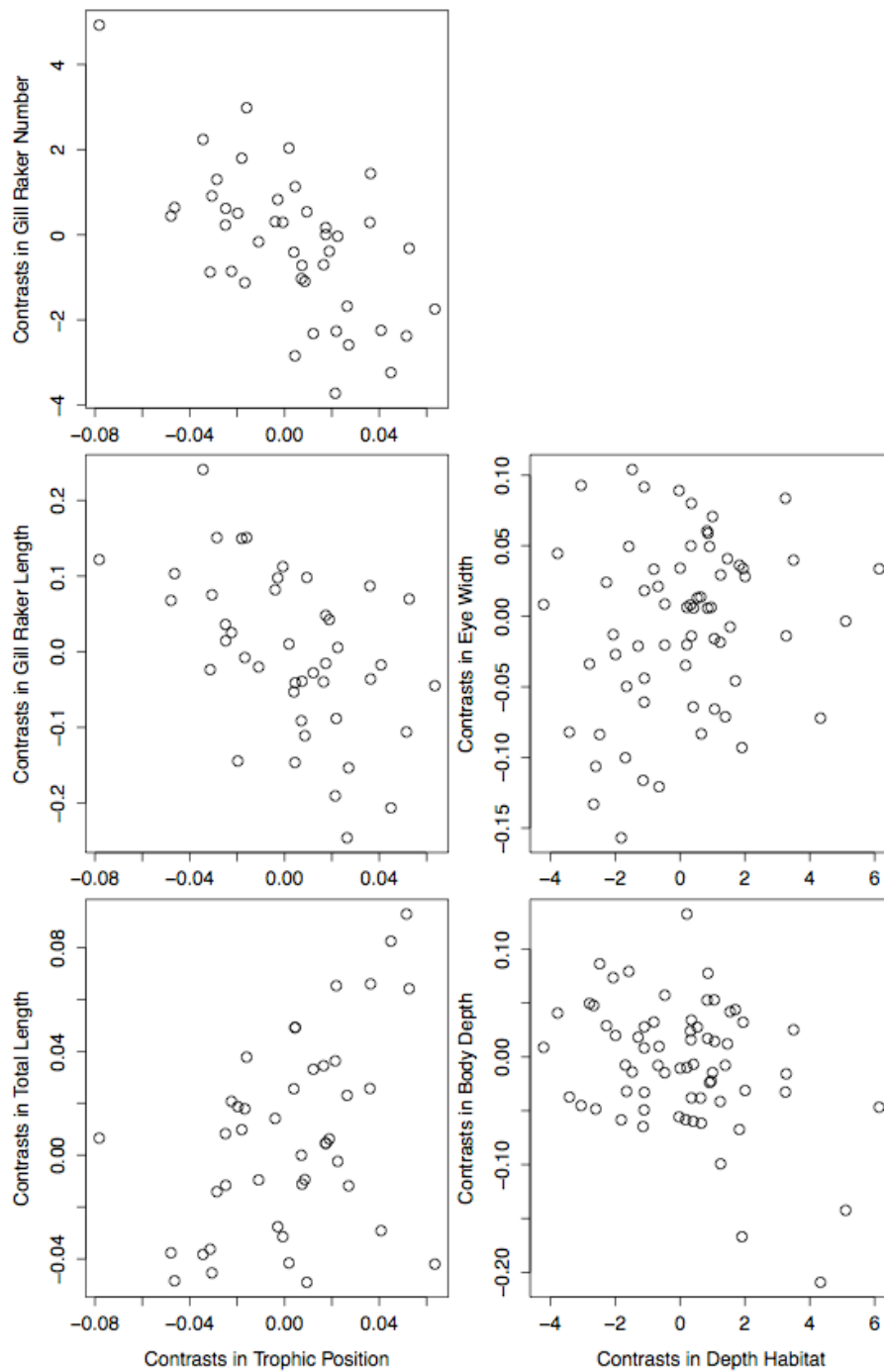
48

49 Figure S1. *Sebastes* phylogeny used for the main analyses presented in this paper. To the  
 50 right of each species' name is its latitudinal (°) and depth (m) ranges. Species not in the  
 51 northeast Pacific dataset are labeled (NWP = Northwest Pacific; A = Atlantic; GC = Gulf  
 52 of California; SH = Southern Hemisphere; X = recently described NEP species, no data).



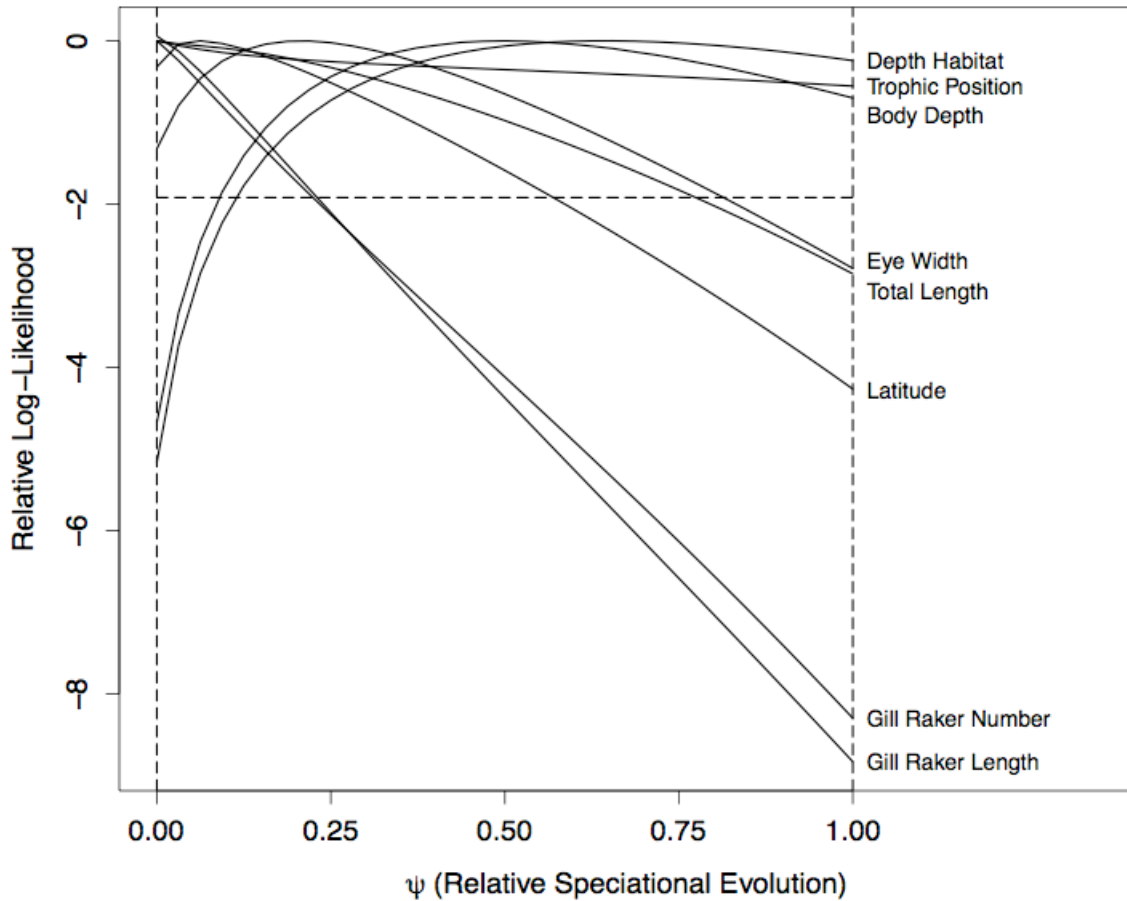
53

54 Figure S2. Asymmetry in range sizes in both latitude and depth, against time since  
 55 divergence for pairs of rockfish species. Asymmetry is calculated following Barraclough  
 56 & Vogler (2000) as (smaller range size)/(sum of range sizes). As in Figure 1, sister  
 57 species are denoted with filled symbols. There was no relationship between asymmetry  
 58 and node age for either latitude (Mantel test,  $p = 0.40$ ) or depth ( $p = 0.56$ ).



59

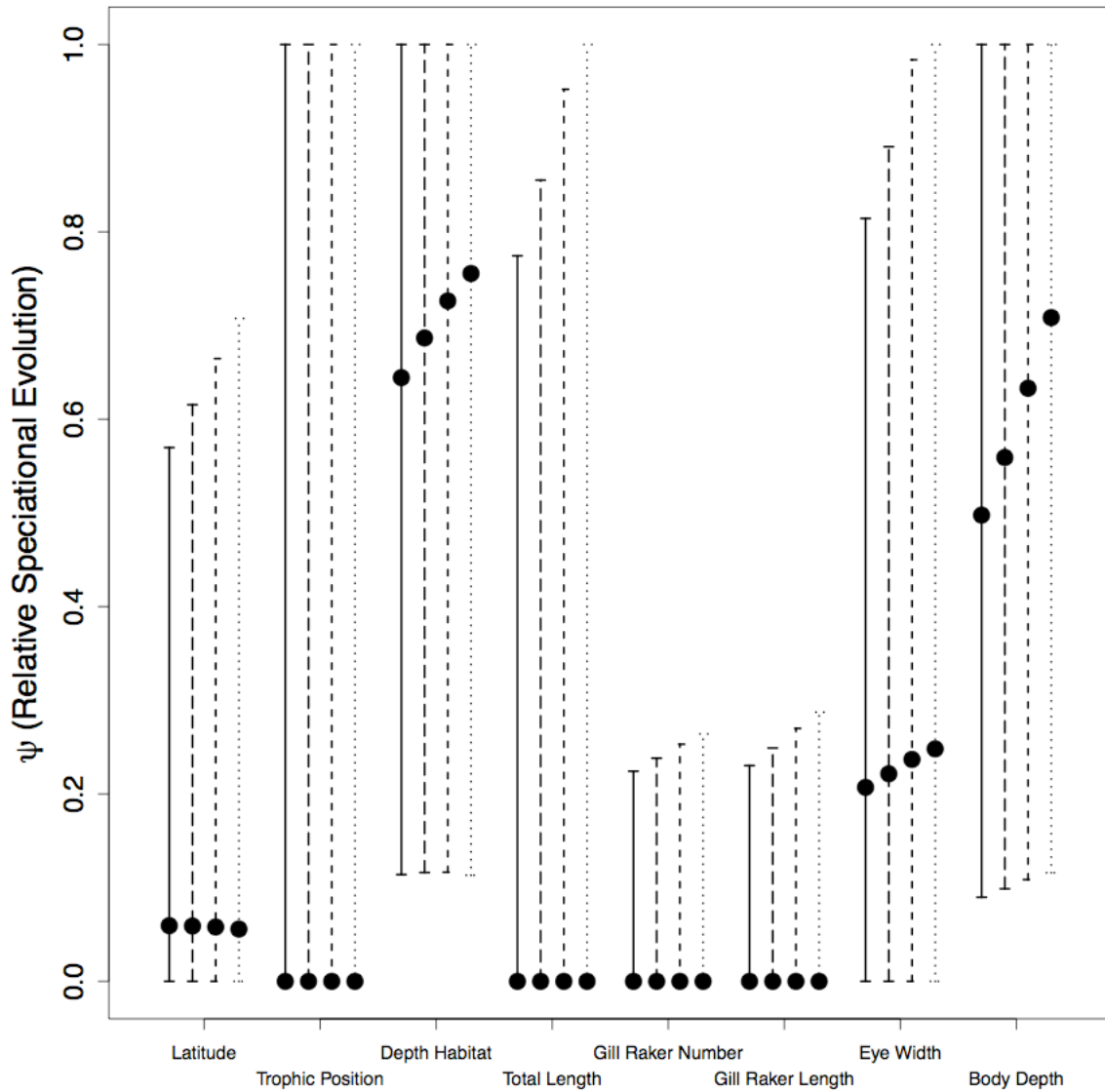
60 Figure S3. Relationships between five morphological traits and the niche axis each is  
 61 most associated with. Phylogenetically independent contrasts in three traits are shown  
 62 against contrasts in trophic position (TP; left column), and contrasts for two traits are  
 63 shown against contrasts in depth habitat (right column).



64

65 Figure S4. Profile likelihood surfaces for  $\psi$  for characters analysed in this study. Log-  
 66 likelihoods were calculated using the maximum likelihood value of  $\sigma^2_t$  corresponding to  
 67 different values of  $\psi$  between the bounds of 0-1, then scaled relative to the maximum  
 68 log-likelihood for each trait. The horizontal dashed line is -1.92, the nominal cutoff for a  
 69 95% confidence interval using a  $\chi^2$  approximation with 1 d.f.

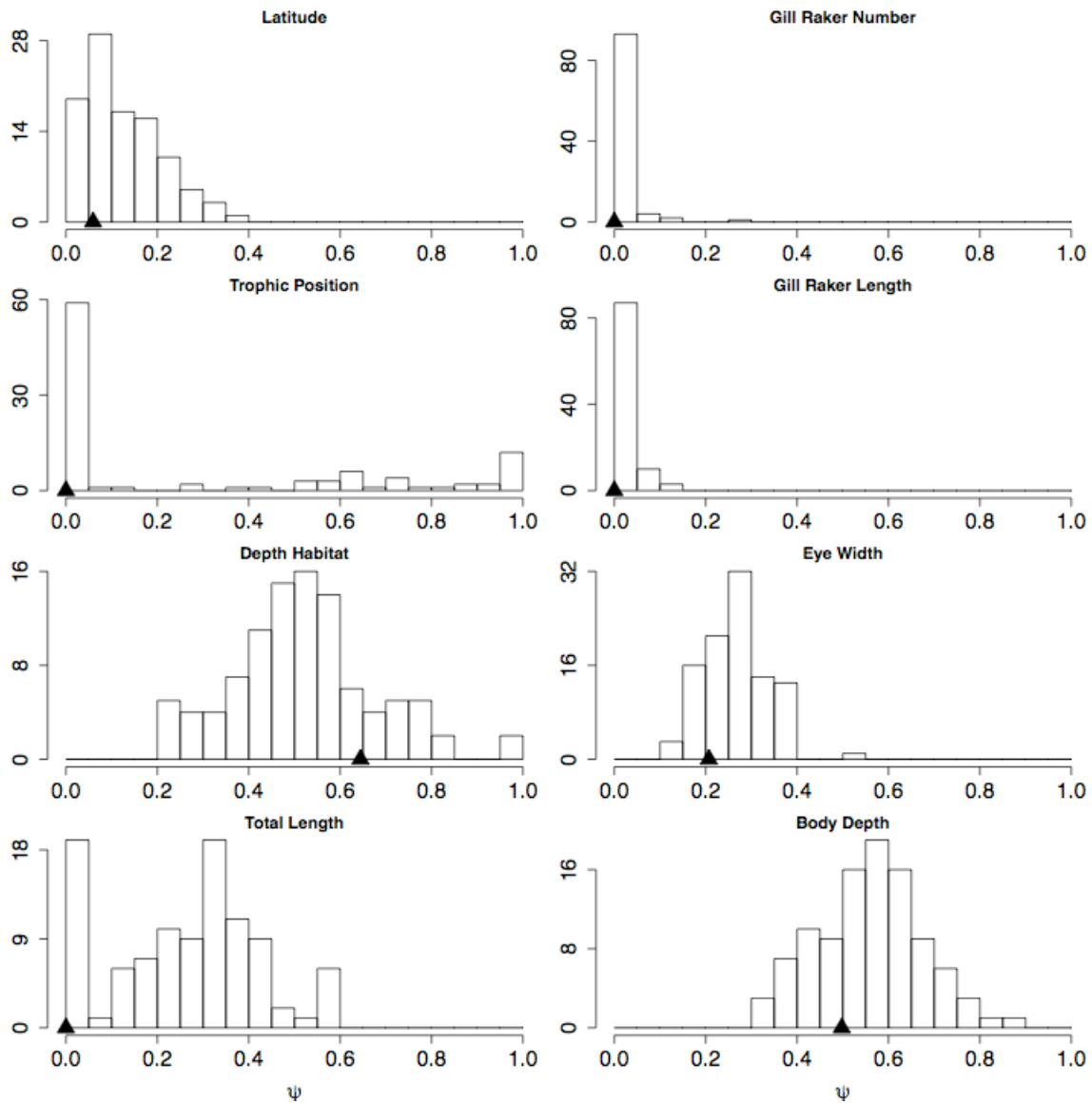
70



71

72 Figure S5. Effect of a non-zero extinction rate on estimation of  $\psi$ . Likelihood analyses of  
 73 speciation evolution in each character were repeated using turnover rates ( $\mu/\lambda$ ) of 0  
 74 (solid line, equivalent to fig. 2), 0.25 (long dashed line), 0.50 (short dashed line) and 0.75  
 75 (dotted line). These turnover rates correspond to values of  $\lambda = 0.35, 0.39, 0.44$  and  $0.47$ ,  
 76 and  $\mu = 0, 0.10, 0.22$  and  $0.35$ , respectively.

77



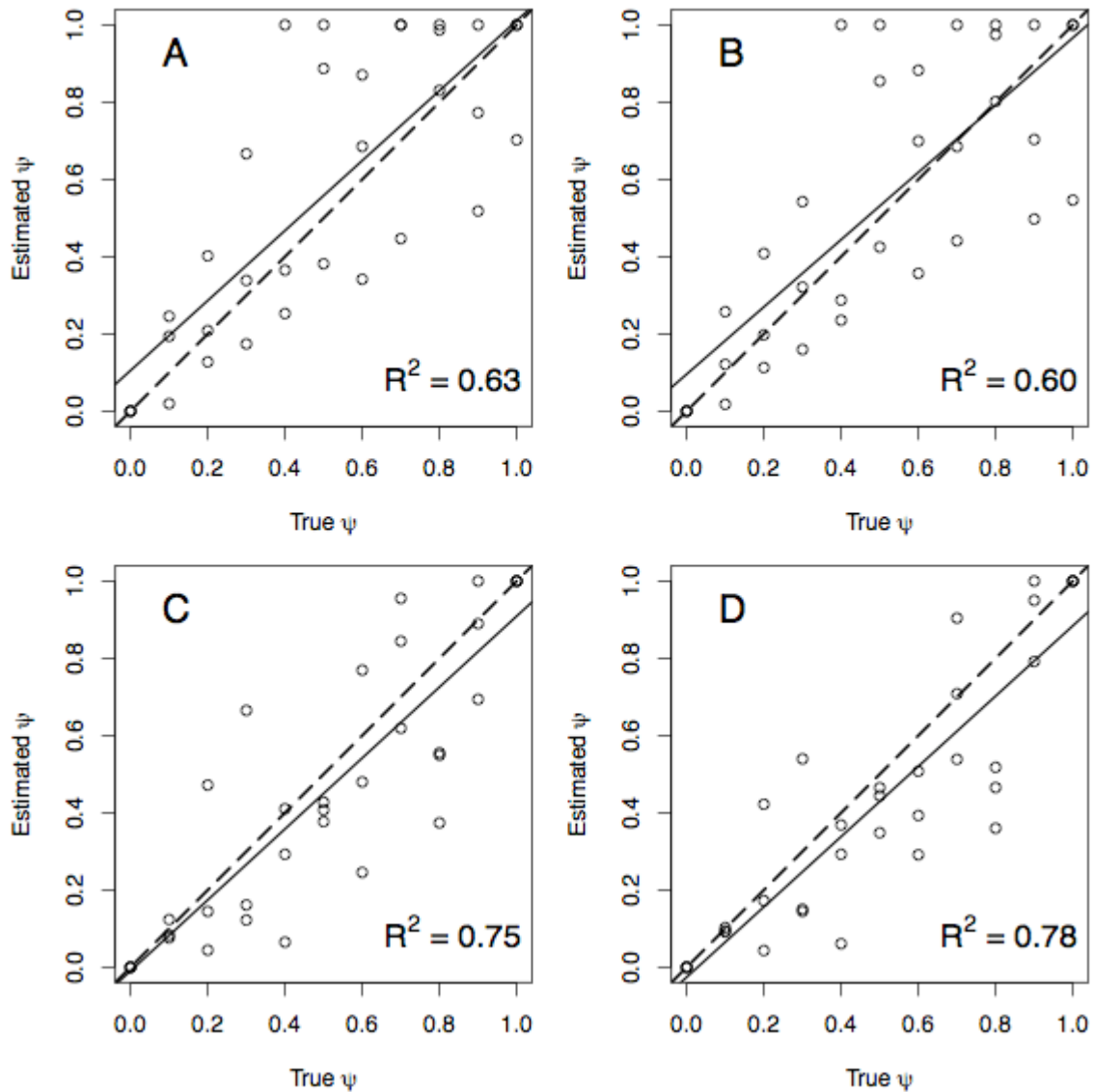
78

79 Figure S6. Distribution of parameter estimates across 100 trees from the posterior sample.

80 For each character, the distributions of the parameter  $\psi$  (relative speciation evolution)

81 are shown. Filled symbols indicate parameter estimates for the maximum clade

82 credibility tree, as shown in fig. 2.



83

84 Figure S7. Recovery of known  $\psi$  values by carrying out maximum likelihood inference  
 85 on simulated phylogenetic trees and trait values. Trees were simulated with no extinction  
 86 ( $\mu = 0$ ; AB) or with  $\mu = 0.1$  (CD).  $\lambda$  and  $\mu$  were either estimated from the phylogeny  
 87 (AC) or their true values were used (BD). Shown in each panel are the 1:1 line (dashed),  
 88 the least-squares regression line of estimated  $\psi$  against true  $\psi$  (solid), and the  $R^2$  for this  
 89 linear fit as a measure of precision.

90